Egyptian Journal of Chemistry

Synthesis of Patchouli Biomass Based Carbon Nanomaterial Using Two Different Double Pyrolysis Methods

Tutik Setianingsih
Department of Chemistry, Brawijaya University, Jl. Veteran 169 Malang 65145, Indonesia

Abstract

Carbon nanomaterial (CNM) is a potential material for many applications such as adsorbent, catalyst, additive of ceramic, electode, etc due to its characteristics. However different pyrolysis methods can affect its properties which affect its performance in application. Therefore purpose of this research is to study influence of the different double pyrolysis methods (reflux - microwave and hydrothermal - microwave) toward properties of the CNM. Patchouli biomass and $ZnCl_2$ was used as the carbon precursor and chemical activator, respectively. The pyrolysis by reflux or hydrothermal method was conducted at 200°C for 6 h, then, each was continued in microwave at 800W for 40 minutes. The products were characterized with FTIR spectrometry, XRD, UV-Vis spectrophotometry, dispersion stability test to achieve main colloidal sol (1-100 nm), and SEM. Results of the research show that the hydrothermal–microwave method produced darker product, higher crystalinity index of cellulose, higher aromaticity, smaller irreguar shape carbon particles (based on SEM), lower content of C-O functional group (based on FTIR spectra), more peaks of UV-Vis spectra, more stable CNM colloid with main content of the colloidal sol (more transparant qualitatively; higher TDS quantitatively) after keeping for 26.75 h, than the reflux– microwave one. However, degree of graphitizations of the carbons which were achieved by both methos were similar.

Keywords: carbon nanomaterial, patchouli biomass, pyrolysis

1. Introduction

Carbon materials can be bulk materials such as biochar and activated carbon or nanomaterials, such as carbon nanotubes, graphene, fullerene, nanodiamond, carbon nanofiber, carbon nanorod, etc. They are interesting research topics due to their unique physico-chemical properties, including high porosity, large surface area, good mechanical resistance, reduced density, excellent electrical and thermal properties [1]. Due to their good properties, carbons material have many potential applications, such as for electrochemical sensor [2], catalyst [3], catalyst matrix [4], and adsorbent [5-7]. Various biomass have been used as precursors of the carbon nanomaterials or composites such as CNM from oil palm [8], CNTs from rice husk [1], plastic waste [9], and from pyrolysis gases of waste polymer such as plastics [10]. Carbon dots from carrot juice [11] and acerola fruit [12], carbon quantum dots from lemon juice [13], and carbon nanosphere from coconut fibre [14]. Biomass of plants are potential carbon precursors due to its carbon content, such as lignin, cellulose, and hemicellulose [15]. Preparation of carbon nano material uses various pyrolysis methods, such as

hydrothermal [16-17], arc-discharge method [18-19] microwave pyrolysis [20], laser ablation and CVD [19]. Hydrothermal pyrolysis tends to use low temperature but involving pressure by autoclave. Microwave pyrolysis involves high temperature and the existence of electromagnetic wave of radiation which can optimize pyrolysis reaction.

In this research, carbon nanomaterial was prepared from patchouli biomass for the purpose of carbon use as additive of liquid fertilizer in a rice field. This research is part of HPU 2019 research project which pyrolyzed three different biomass by hydrothermal - microwave and reflux - microwave, including patchouli biomass, rice husk, and sugarcane leaf. Nanomaterial is considered to make spraying easier due to the existence of carbon as dispersion [22]. Nanomaterial in which size of less than 100 nm is dispersed in fluids such as water [21].

Novelty of this research is that this research can show effect of the different pyrolysis method combination toward concentration of the carbon colloid qualitatively and quantitatively. These properties are important in application of carbon nanomaterial in agriculture, especially as additive of

the fertilizer solution so that it needs the requirement as dispersion to make easy sprayng.

Goal of this research to study influence of different pyrolysis method combinations or double pyrolysis methods (reflux-microwave and hydrothermal-microwave) toward properties of CNM from patchouli biomass using $ZnCl_2$ chemical activator .

2. Experimental

2.1. Synthesis of carbon nanomaterial from patchouli biomass [22]

This erxperiment used a raw materal, patchouli biomass or nilam (N), including stem and root mixture from patchouli oil destilation home industry Batu Malang, after cleaning, drying, milling, and shieving to get particle size > 60 mesh. $ZnCl_2$ (Merck) was used as chemical activator in pyrolysis, and destilated water as solvent.

A mixture consisting of 50 g of patchouli biomass or nilam (N), 1 gram of $ZnCl_2$, and 100 mL of distilled water was refluxed at 200ºC for 6 h using the boiled coconut oil heater. The product was pyrolyzed again by microwave oven at 800 W or 40 minutes. Code of the pyrolyzed carbon using reflux - microwave method is NR200-MC40.

Another mixture was prepared, including biomass (10 g), $ZnCl_2$ (0.2 g), and water (20 mL), then pyrolized at 200ºC hydrothermally for 6 h. Further pyrolysis was conducted using microwave for 40 minutes at 800 W. Code of the carbon which was produced by pyrolysis using hydrothermal - microwave is NH200-MC40.

Instruments for hydrothermal and microwave pyrolysis are same with the ones shown in other research [23] due to same part of HPU 2019 research project.

2.2. Characterization

The carbon products were characterized with FTIR spectometer at a range of 400 – 4000 cm^{-1} using KBr pellet to characterize surface functional groups.

Biomass and the carbons were characterized using X-ray diffraction (PANalitical type XPert PRO), with Cu-Kα (λ=1.54021 Å) at a range of 2θ = 10 to 80º, 40 kV, 35 mA with a scan step time of 0.7 seconds. Crystallinity index was calculated using this formula 1 [24] :

$$Cr.I. = I_{200} - I_{am} \text{ X } 100\% / I_{200} \quad (1)$$

I_{200} presents the highest peak intensity with hkl of (200) at 2θ of 22º and I_{am} is the intensity at 2θ of 18°, related to amorphous structure.

Aromaticity (f_a) is ratio of the aromatic atom C and total atom C (the aromatic atom C + the aliphatic atom C). Theoretically, area of π peak (d_{002}) at 26° is equivalent to number of aromatic carbon atoms (C_{ar}) and area of the γ peak (20°) is equivalent to number of the aliphatic carbon atom (C_{al}) [25]. By assumption that the baseline length of each π and γ peak is same,

the peak area can be substituted by peak intensity (I), so that aromatocity of the carbon can be calculated by formula 2 :

$$f_a = C_{ar} / [C_{ar} + C_{al}] = I_{002}/(I_{002} + I_\gamma) \quad (2)$$

Degree of graphytization is calculated based on data of intensity using formula 3 :

$$g = [I_{002}/I_{10} \text{ X } 100\%] / 14.3 \quad (3)$$

I_{002} and I_{10} is peak of X-ray diffraction with hkl = 002 and 10, respectively. Number of 14.3 is related to the perfect pyrolytic graphitized carbon without amorphous phase [26].

SEM was used to characterize the topography morphology of the carbon surface. Topography includes fiture (appearance) and texture. Morphology includes size, shape, and distribution of particles.

To measure UV-Vis spectra of the colloid, the carbon product (2 g) was immersed in water (50 mL) and were stirred using a magnetic stirrer for 1 h. Then, each colloid (5 mL) was mixed with the destilled water at volume ratio of 1:1, shaken by hand for several times, and measured with UV-Vis spectrophotometer (Shimadzu).

To perform test of colloid stability, the mixtures of CNM (0.5 g) and water (50 mL) were blended for 1 h and 30 min using blender (Matsunichi, MSI-T2GN, RRC). The colloids were observed qualitatively at 0 h, 13.25 h (from 04.15 AM - 17.30 PM), and 26.75 h (from 04.15 AM to the next day at 06.35 AM] using a digital camera (CANON PowerShot SX430 IS; Wuxi; RRC) from the opposite side of sunlight and flash light. Quantitatively, concentration of the colloids were measured using TDS meter [mini water quality tester mutlifunction].

3. Result and Discussion

3.1. Changing of color

The patchouli biomass [Figure 1] has been used as a carbon nanomaterial precursor. Based on analysis by analysis laboratory of Chemistry Department Brawijaya University, the patchouli biomass contains 18.72 ± 0.90% of hemicellulose, 29.45 ± 0.74% of lignin, and 42.1 ± 9.82% of cellulose. Based on those all chemical structures [27], the patchouli biomass is rich of aromatic structures from lignin and rich of both -OH and C-O-C groups from all those substances.

In this research, these aromatic structures were improved by different pyrolysis methods to form graphene layers which construct the carbon. Improving these structures gave consequence on changing of material color from light brown of the biomass to black color of the carbon. Figure 2 shows the changing of colors from biomass to carbon products for each pyrolysis method.
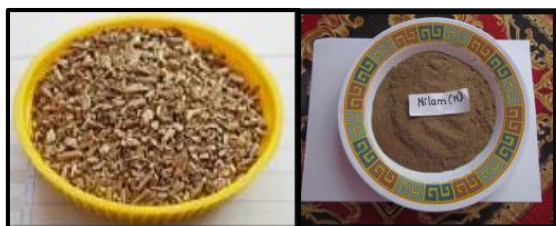
_____

Figure 1. Patchouli biomass (N)

Figure 2. Biomass (N) and the carbon from pyrolysis of patchouli biomass using reflux–microwave (NR200-MC40) and hydrothermal–microwave (NH200-MC40).

The chemical reactions which are related to pyrolysis of each lignin, hemicellulose, and cellulose were predicted in other research [28]. Along pyrolysis reaction, $ZnCl_2$ has the role as dehydrating agent which improve the carbonization and prevent tar [29]. $ZnCl_2$ also acts as the pore template which controles both pore structure and size [30].

Microwave pyrolysis made the carbon darker than after hydrothermal or reflux pyrolysis. It indicates that the microwave pyrolysis has completed the carbonization reaction of the biomass. Beside that, there were some aglomerates in the product after hydrothermal and reflux microwave. This is because both methods were handled in low temperature so that the product still contained the hydrate which created some agglomerated particles of the products. Those agglomerates were removed again after microwave pyrolysis due to more carbonization reaction and evaporation of the hydrates.

3.2. Functional groups
To identify possibility of functional groups differences due to different pyrolysis, characterization using FTIR spectrometry was conducted and reported in Figure 3. Only the FTIR spectra of the final products (NR200-MC40 and NH200-MC40) were considered for compared to the spectrum of the patchouli biomass or nilam (N).

Figure 3 shows that pyrolysis of the biomass causes FTIR bands weakening at about 3400, 2900, and 1050 cm^{-1} connected to -OH (hydrate or phenolic), –CH aliphatics, and C-O functional groups, respectively.

The bands at about 1650 cm^{-1} are vibration of C=C, This bands become sharper by single method of pyrolisis but weaker again by double method of pyrolisis. The band between 500 and 600 cm^{-1} is vibration of M-O. It is similar to peak of Fe-O at 549 cm^{-1} [31].
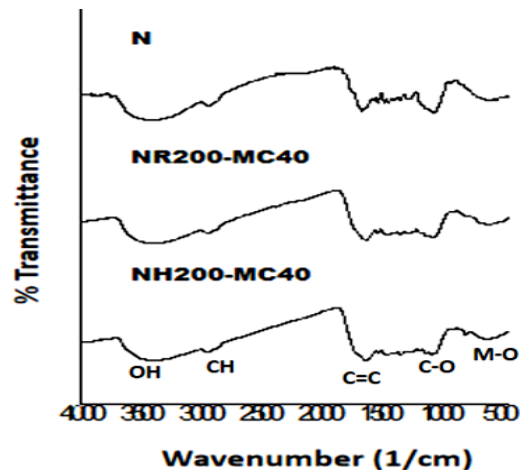

Figure 3. FTIR spectra of the carbon from pyrolysis of patchouli biomass using reflux – microwave (NR200-MC40) and hydrothermal – microwave (NH200-MC40).

In other side, the C=C aromatics become sharper in sequence of NH200-MC40 > NR200-MC40 > N. It indicates more aromatics structures in graphene layers of the carbon. This band can be detected due to oxy functional groups on edges of the graphene which created unsymetric environment for the C=C aromatics.

3.3. Crystal structure
Crystal structure of the carbons were characterized with XRD as presented in Figure 4. Beside the codes of the samples given by ourselves, we also gave other codes (in the bracket) from LSUM Malang State University, where the XRD characterization was conducted.
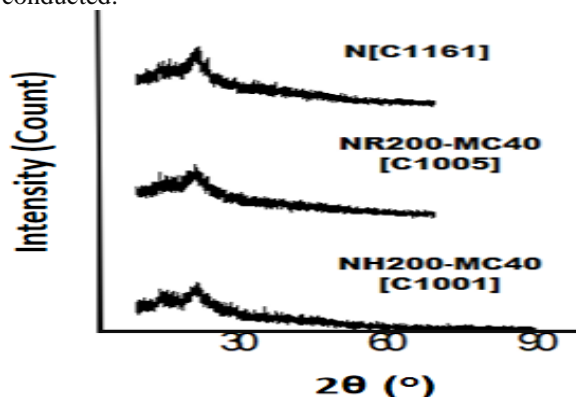

Figure 4. X-ray diffractogram of the carbon from pyrolysis of the patchouli biomass using the reflux–microwave methods (NR200-MC40) and hydrothermal–microwave methods (NH200-MC40).

Patterns of the difractograms indicate crystal structure like cellulose fiber [32], CNT [33], and CND [3]. Based on the crystalinity index of cellulose, it is known that the the CNM which was prepared by reflux - microwave pyrolysis [NR200-MC40] had lower crystalinity index of cellulose than the biomass (N). It indicates damage of cellulose structure due to carbonization reaction. However, Data in Table 1 shows higher crystalinity index of cellulose for the CNM after hydrothermal - microwave pyrolysis of biomass (NH200-MC400). It indicates formation of the carbon phase with same structure with cellulose crystal.

Table 1. Crystalinity Index of cellulose (CI%) in patchouli biomass and CNM

Sample	$I(2\theta = 22^o)$	$I(2\theta = 18^o)$	CI(%)
N	3.0	1.4	53
NR200-MC40	1.8	0.9	50
NH200-MC40	1.6	0.7	56

Data aromaticity in Table 2 shows that both CNMs have higher aromaticity than biomass(N). This parameter describes the aromatic strctures which were formed in pyrolysis process relative to total alyphatic and aromatic carbon structures. Both carbons have higher aromaticity indicating the improvement of the aromatic structures formed due to pyrolysis reactions. The NH200-MC40 has higher aromaticity probably due to higher pressure pyrolysis which made more completed pyrolysis reaction.

Table 2. Aromaticity of the biomass and the CNM

	I_{002} $(2\theta= 26^o)$	I_γ $(2\theta=20^o)$	f_a
N	1.2	2.4	0.33
NR200-MC40	1.4	2.5	0.36
NH200-MC40	1.7	2.5	0.41

The graphite structure consists of stack of layer planars called graphene layers. Each layer is constructed by many adjacent aromatic structures and between each 2 graphene layers were separated by at 3.35 Å and held by a weak attraction force named Van der Waals [34]. Degree of graphitization describes crystality of the graphite structure in the carbon product. Tabel 3 presents data of degree of graphitization for the biomass (N) and the carbons (NH200-MC40 and NR200-MC40). Both carbons have higher degree of graphitizations. It means that along pyrolysis reactions formation of graphite structures were lasted. However both carbons have only litle different degree of graphitization and it can be assumed as similar as about 24 %.

Table 3. Degree of graphitization for biomass and the CNM

	I_{002} $(2\theta = 26^o)$	I_{10} $(2\theta = 43^o)$	g (%)
N	1.2	0.5	16.78
NR200-MC40	1.4	0.4	24.48
NH200-MC40	1.7	0.5	23.78

3.4. Morphology of CNM

Morphology of carbon was characterized by SEM in Figure 5. Those SEM images show that the carbon synthesized by hydrothermal – microwave methods has smaller solid particles than by the reflux-microwave ones. It is due to higher pressure in the hydrothermal - pyrolysis methods than in the reflux - microwave ones.

Higher pressure in the aotoclave is caused by the autoclave which is constructed by the closed thick stanless and teflone. This closed condition causes the emitted vapour along pyrolysis reaction can't be removed and create high pressure in the autoclave. This pressure help to destroy chemical bonding along reaction and conditionize the product to smaller size of particles. In other side, the pressure in the flash of reflux apparatus is lower due to coolling by condensor which changes the vapour to the liquid again so that the pressure in the flash can be reduced.
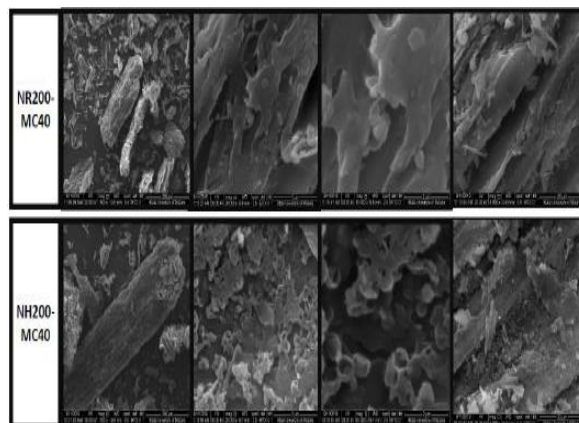
Figure 5. X-ray diffractogram of the carbon from pyrolysis of the patchouli biomass using the reflux–microwave methods (NR200-MC40) and hydrothermal–microwave methods (NH200-MC40).

3.5. UV-Vis spectra of the CNM colloids

Colloid is combination of the particles as the dispersed phase and solven as the medium phase. Essentially, particle size of the colloidal sol system (1-100 nm) is different from the particles of both the suspension system (> 100 nm) and the solution (< 1 nm) [35]. It means that nanomaterial is included in the colloidal sol groups. Therefore, the nanomaterial can be characterized with dispersion test. However, There

is other reference which classifies 3 kinds of the dispersion systems, including molecular dispersion (<1 nm), colloidal dispersion (1-500 nm), and coarse dispersion (> 500 nm) [36].

The prepared CNM colloid can measured with UV-Vis spectrometer to identify C=C bond and C=O bonds in the carbon. Both colloids and UV-Vis spectra of the CNMs are presented in Figure 6.
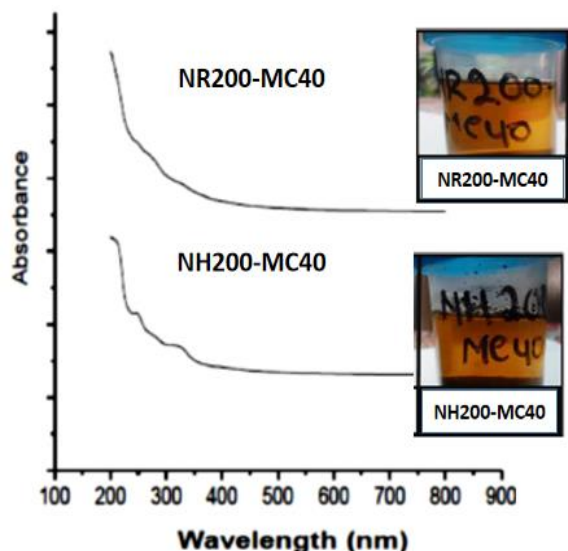

Figure 6. UV-Vis spectra of the carbon collids from pyrolysis of patchouli biomass using reflux – microwave (NR200-MC40) and hydrothermal – microwave (NH200-MC40).

Spectra of the colloid was measured by UV – Vis spectrophotometry as showed in Figure 5. The carbon produced by hydrothermal – microwave shows 2 peaks at 265.5 and 329.9 nm. In other side, the carbon resulted by reflux – microwave method has only shoulder at 265.5 nm. The peak at 265.5 nm indicates π-π* transitions of the C=C bond in aromatics structure. This peak is little smaller than 275 nm [20]. This peak. This shift can be caused by existence of oxy-functional groups of the carbon. The peak at 329.5 nm is closer to 343 nm connected to vibration of C=O n-π* transition [23].

3.5. Test of colloid stability

There are different physical properties of the different colloid class. This differences were used as base for identify the colloid stability.

The appearance of the colloidal sol and the solution are transparant, but the suspension is opaque. The solution doesn't settle down, the colloidal sol settles down by centrifugation, and the suspension settles down by itself [35]. The appearance of them including transparant, opalescent, and opaque, respetivle. Both molecular dispersion and colloidal sol don't settle down, but the coarse dispersion settles down by gravitation and other force [36].

Stabilities of carbon colloids were observed 3 times, including 0 h (starting time), after keeping for 13.25 h and after keeping for 26.75 h. The starting time was observed after reshaking several times of the colloids which have been formed previously by blending to re-create the most dark colloids as shown in Figure 7.

Figure 7. The colloid of CNMs from patchouli biomass by hydrothermal - microwave (NH200-MC40) and reflux - microwave (NR200-MC40) methods after blending process for 30 minutes (B30) and 60 minutes (B60) under sunshine and the flah light.

All colloids show dark or black color which indicate presence of both coarse and colloidal dispersion mixture. However, although they look same dark but the TDS measurement provided the different values. The TDS measurement process was conducted as shown in Figure 8.

Figure 9 shows TDS of the CNM colloids which were taken from different pyrolysis (NR200-MC40 and NH200-MC40) and different time of blending proccess, including 60 minute (B60) and 30 minutes (B30). Figure 9 shows that for 30 minutes of blending (B30), the NR200-MC400 carbon has higher TDS than NH200-MC40, but for 60 minutes of blending, the NH200-MC40 has the higher TDS than NR200-MC40.

Figure 9 shows that the blending for 60 minutes (B60) gave higher TDS for both NR200-MC40 and NH200-MC40 colloids than the 30 minute blending. This is probably due to higher colloidal dispersion in the colloids which were taken by longer blending. Higher colloidal dispersion can prevent sedimentation than the coarse dispersion due to smaller particles.

_____

Based on Newton law, bigger particles are attracted stronger by gravitation force of the earth [37].
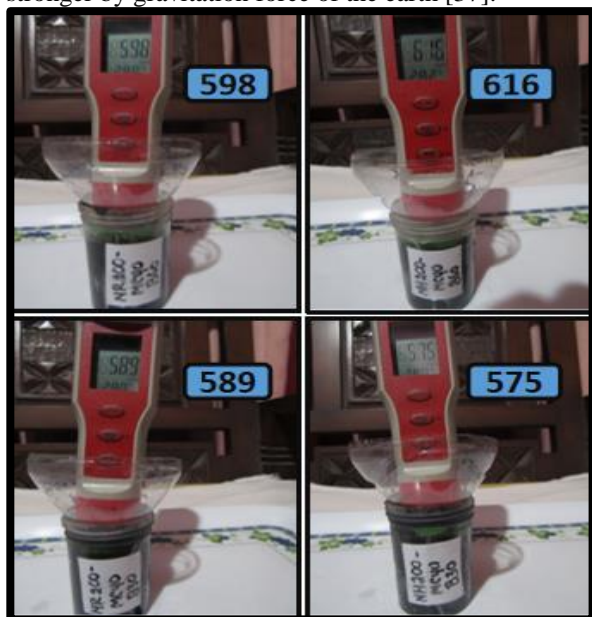

Figure 8. TDS measurement process for the colloid of CNMs from patchouli biomass by hydrothermal - microwave methods (NH200-MC40) and reflux - microwave methods (NR200-MC40) methods after blending process for 30 minutes (B30) and 60 minutes (B60).
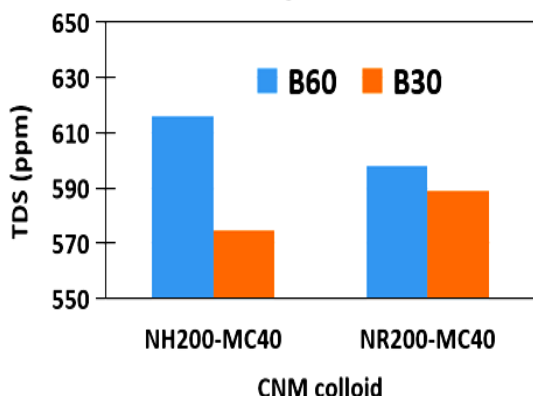

Figure 9. TDS of CNM colloids from patchouli biomass by hydrothermal - microwave (NH200-MC40) and reflux - microwave (NR200-MC40) methods after blending process for 30 minutes (B30) and 60 minutes (B60).

However, there is interesting phenomenon from this observation. For 60 minute blending (B60), NH200-MC40 has higher TDS than NR200-MC40, but for 30 minute blending (B30), oppositely colloid of NR200-MC40 has higher TDS than NH20-MC40. It is no question if NH200-MC40 has higher TDS than NR200-MC40 after blending for 60 minutes, it is exactly due to not only smaller particles by higher pressure pyrolysis methods but also longer breaking process of particles by blending.

However, if NR200-MC40 has higher TDS than NH200-MC40 after 30 minutes blending, there is another factor which controls it. It is probably related to their functional groups. Based on their FTIR spectra, NR200-MC40 has more C-O surface functional groups than NH200-MC40. This C-O group has Lewis base O which can make hydrogen bonding with positive dipoles of the H_2O molecules or of polar groups such as -OH on the CNM particles surface. More force attraction of dipole of H_2O and C-O of the NR200-MC40 probably can cause more particles of the NR200-MC40 can be sustained as dispersion than of the NH200-MC40 toward effect of gravitation. However, after 60 minutes blending and the colloidal dispersion have been improved, the effect of higher colloidal sol concentration dominates sustainability of the colloid than effect of the C-O groups of the carbon.

The colloids after keeping 13. 25 h and 26.75 h are presented in Figure 10 and 11, respectively. Figure 10 shows color of brown opalescent and yellow transparant. This is different from the colors of the coloids at starting time which show black for all the colloids. It indicates that after keeping for 13.25 h some particles settled down on the bottom. These settled down particles are coarse dispesion particles. After keeping for 26.75 h, the colloids in Figure 11 look more transparant than the colloids in Figure 10. It indicates more settling down of the coarse particles by longer keeping time.

Figure 10. The colloid of CNMs from patchouli biomass by hydrothermal - microwave (NH200-MC40) and reflux - microwave (NR200-MC40) methods after blending process for 30 minutes (B30) and 60 minutes (B60) under the flah light after keeping

_____

for 13.25 h.

Figure 11. The colloid of CNMs from patchouli biomass by hydrothermal - microwave (NH200-MC40) and reflux - microwave (NR200-MC40) methods after blending process for 30 minutes (B30) and 60 minutes (B60) under the flah light after keeping for 26.75 h.

Figure 12 shows proccess of TDS measurement toward the colloids after keeping for 26.75 h. Figure 13 shows that TDS of the NH200-MC40 is higher than the NR200-MC40 for blending proccess for both 30 minutes (B30) and 60 minutes (B60). The colloid of NH200-MC40 (B60) is the most transparant and has yellow color and has the highest TDS. It indicates that the colloid of NH200-MC40 is mainly about collodal sol. This condition is caused by factors, including hydrothermal pyrolysis which involved higher pressure than reflux one. The other factor is longer time of blending proccess which caused more particles can be broken to smaller ones.

The others are brown opalescent, indicating that the colloids still contain coarse colloid but much lower than the starting colloids. Among the three colloids, the intensity of brown color increases by sequence of NR200-MC40 (B30) < NR200-MC40 (B60) < NH200-MC40 (B30). This sequence is match with the TDS values. It means that the TDS is supported by the coarse dispersion and colloidal sol particles with the mainly colloidal sol.

Figure 13. TDS of CNM colloids from patchouli biomass by hydrothermal - microwave (NH200-MC40) and reflux - microwave (NR200-MC40) methods after blending process for 30 minutes (B30) and 60 minutes (B60) after keeping 26.75 h.

Figure 12. TDS measurement process for the colloid of CNMs from patchouli biomass by hydrothermal - microwave (NH200-MC40) and reflux - microwave (NR200-MC40) methods after blending process for 30 minutes (B30) and 60 minutes (B60) after keeping for 26.75 h.
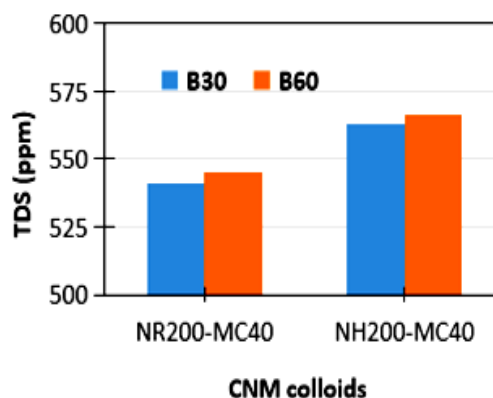
4. Conclusions

Pyrolysis of patchouli biomass has been conducted by 2 different double pyrolysis methods, including reflux - microwave methods and hydrothermal - microwave methods. The hydrothermal – microwave method resulted in the darker carbon, higher crystalinity index of cellulose, higher aromaticity, smaller irregular solid particles based on SEM images, more stable colloid with main content of colloidal sol (1-100 nm), little lower content of C-O (based on FTIR spectra), and more peaks of UV-Vis spectra and than the reflux - microwave method. However, degree of graphitization of both carbons were similar.

5. Acknowledgement

_____

6. Conflicts of interest

There are no conflicts to declare.

References

[1] Asnawi, M., Azhari , S., Hamidon, M.N., Ismail, I., & Helina, I., Synthesis of Carbon Nanomaterials from Rice Husk via Microwave Oven. *Hindawi Journal of Nanomaterials, vol. 2018*, 1-5 (2018). https://doi.org/10.1155/2018/2898326

[2] Seo, D.H., Pineda, S., Fang, J., Gozukara, Y., Yick, S., Bendavid, A., Lam, S.K.H., Murdock, A.T., Murphy, A.B., Han, Z.J., & Ostrikov, K., Single-step Ambient-air Synthesis of Grapheme from Renewable Precursors as Electrochemical Genosensor. *Nature Communications*, *8* (14217), 1-9 (2017). DOI: 10.1038/ncomms14217\

[3] Haryadi, Purnama, M.R.W., & Wibowo, A., C Dots Derived from Waste of Biomass and Their Photocatalytic Activities. *Indones. J. Chem., 18* (4), 594 – 599 (2018). DOI: 10.22146/ijc.26652

[4] Wu, S., and Dai, W., Microwave-Hydrothermal Synthesis of SnO_2 - CNTs Hybrid Nano composites with Visible Light Photocatalytic Activity. *Nanomaterials, 7* (54), 1-7 (2017). doi:10.3390/nano7030054

[5] Bahrami, M., Amiri, M.J., and Koochaki, S., Removal of Caffeine from Aqueous Solution Using Multi-wall Carbon Nanotubes: Kinetic, Isotherm, and Thermodynamics Studies. *Pollution, 3*(4), 539-552 (2017). DOI: 10.22059/POLL.2017.62771

[6] Shan, J., Ji, R., Yu, Y., Xie, Z., & Yan, X., Biochar, Activated Carbon, and Carbon Nanotubes Have Different Effects on Fate of 14C-catechol and Microbial Community in Soil. *Scientific Reports, 5*(16000), 1-11 (2015). DOI: 10.1038/srep16000

[7] Sweetman, M.J., May, S., Mebberson, N., Pendleton, P., Vasilev, K., Plush, S.E., and Hayball, J.D., Review: Activated Carbon, Carbon Nanotubes and Graphene: Materials and Composites for Advanced Water Purification. *Journal of Carbon Research, 3*(18), 1-29 (2017). doi:10.3390/c3020018

[8] Nasir, S., Hussein, M.Z., Zainal, Z., Yusof, N.A., Zobir, S.A.M., and Alibe, I.M., Liotta,F., Potential Valorization of By-product Materials from Oil Palm: A review of Alternative and Sustainable Carbon Sources for Carbon-based Nanomaterials Synthesis. *BioResources, 14*(1), 1-37 (2018). DOI: 10.15376/biores.14.1.Nasir

[9] Jia, Z., Kou, K., Qin, M., Wu, H., Puleo, F.L., Controllable and Large-Scale Synthesis of Carbon Nanostructures: A Review on Bamboo-Like Nanotubes. *Catalysts, 7*(256), 1-21 (2017). doi:10.3390/catal7090256

[10] Borsodi, N., Szentes, A., Miskolczi, N., Wu, C., Liu, X., Carbon Nanotubes Synthetized from Gaseous Products of Waste Polymer Pyrolysis and Their Application. *Journal of Analytical and Applied Pyrolysis, 120*, 304-313 (2016). https://doi.org/10.1016/j.jaap.2016.05.018

[11] Liu, Y., Liu, Y., Park, M., Park, S.J., Zhang, Y., Akanda, M.R., Park, B.Y., and Kim, H.Y., Green Synthesis of Fluorescent Carbon Dots From Carrot Juice For In Vitro Cellular Imaging. *Carbon Letters, 21,* 61-67 (2017). http://dx.doi.org/10.5714/CL.2017.21.061

[12] Carvalho, J., Santosa, L.R., Germino, J.C., Terezoa, A.J., Hydrothermal Synthesis to Water-stable Luminescent Carbon Dots from Acerola Fruit for Photoluminescent Composites Preparation and its Application as Sensors, *Materials Research, 22*(3), 1-8 (2019). http://dx.doi.org/10.1590/1980-5373-MR-2018-0920

[13] Hoan, B.T., Tam, P.D., and Pham, V.H., Green Synthesis of Highly Luminescent Carbon Quantum Dots from Lemon Juice, *Hindawi Journal of Nanotechnology, Vol. 2019*, 1-9 (2019). https://doi.org/10.1155/2019/2852816

[14] Adewumi, G.A., Revaprasadu, N., Eloka-Eboka, A.C., Inambao, F.L., and Gervas, C., *In Proceedings of the World Congress on Engineering and Computer Science (WCECS) II:* A Facile Low-cost Synthesis of Carbon Nanosphere from Coconut Fibre, San Francisco, USA (2017). http://www.iaeng.org/publication/WCECS2017/ WCECS2017_pp577-582.pdf

[15] Liu, Y., Chen, J., Cui, B., Yin, P., and Zhang, C., Design and Preparation of Biomass-Derived Carbon Materials for Supercapacitors: A Review, *Journal of Carbon research, 4*(53), 1-32 (2018). doi:10.3390/c4040053

[16] Razali, M.H., Ahmad, A., Azaman, M.A., Amin, K.A.M., Physicochemical Properties of Carbon Nanotubes (CNT's) Synthesized at Low Temperature using Simple Hydrothermal Method, *International Journal of Applied Chemistry, 12*(3), 273-280 (2016). https://www.ripublication.com/ijac16/ijacv12n3_10.pdf

[17] Hu, B., Wang, K., Wu, L., Yu, SH., Antonietti,M., and Titirici, M.M., Engineering Carbon Materials from the Hydrothermal Carbonization Process of Biomass, *Adv. Mater., 22*, 813–828 (2010). DOI: 10.1002/adma.200902812

[18] Flygare, M., Svensson, K., Quantifying Crystallinity in Carbon Nanotubes and Its Influence on Mechanical Behavior, *Materials Today Communications, 18*, 39–45 (2019). https://doi.org/10.1016/j.mtcomm.2018.11.003

[19] Szabó, A., Perri, C., Csató, A., Giordano, G.,

_____

_____

Vuono, D., and Nagy, J.B., Review: Synthesis Methods of Carbon Nanotubes and Related Materials, *Materials, 3,* 3092 - 3140 (2010). doi:10.3390/ma3053092

[20] Roshni, V. and Divya, O., One-step Microwave-assisted Green Synthesis of Luminescent N-doped Carbon Dots from Sesame Seeds for Selective Sensing of Fe(III), *Current Science, 112* (2), 385-390 (2017).

doi: 10.18520/cs/v112/i02/385-390

[21] Mahbubul, M., Chong, T.H. Khaleduzzaman, S.S. Shahrul, I.M.. Saidur, R. Long, B.D. and Amalina, M.A., Effect of Ultrasonication Duration on Colloidal Structure and Viscosity of Alumina−Water Nanofluid I. *Ind. Eng. Chem. Res*. **53**, 6677−6684 (2014).

https://doi.org/10.1021/ie500705j

[22] Setianingsih, T., Mutrofin, S. Sintesis Karbon Nanomaterial dari Limbah Biomassa yang Dimodifikasi MFe_2O_4 Secara Green Technology Sebagai Campuran Pupuk Cair Untuk Remediator Tanah Sawah dan Saluran Irigasi Tercemar Pestisida, Laporan akhir HPU, Universitas Brawijaya, Malang (2019).

[23] Setianingsih, T., Susilo, B., Mutrofin,S., Ismuyanto, B., Endaryana, A.N.Yoniansyah, Y.N., Synthesis of MFe_2O_4/CNS (M = Zn, Ni, Mn) Composites Derived from Rice Husk By Hydrothermal - Microwave Method for Remediation of Paddy Field, *Processes, 9*(8), 1349 http://doi.org/10.3390/pr9081349

[24] Poletto, M., Pistor, V., & Zattera, A.J. Structural Characteristics and Thermal Properties of Native Cellulose, Chapter 2, InTech, 45-68 (2013).

doi: 10.5772/50452

[25] Manoj, B and Kunjomana, A.G., Study of Stacking Structure of Amorphous Carbon by X-ray Diffraction Technique, *Int J Electrochem Sci, 7*(4), 3127–3134 (2012).

https://www.researchgate.net/publication/267722188 _Study_of_Stacking_Structure_of_Amorphous_C arbon_by_X-Ray_Diffraction_Technique

[26] Lätt, M., Käärik, M., Permann, L., Kuura, H., Arulepp, M., Leis, J., A Structural Influence on The Electrical Double - Layer Characteristics of Al_4C_3-derived Carbon, *J. Solid State Electrochem*., **14**(4), 543–548 (2010).

https://doi.org/10.1007/s10008-008-0659-3

[27] Setianingsih, T., Masruri, Ismuyanto,B., Biochar and Functionalization of Biochar, UB Press, Malang (2018).

https://books.google.co.id/books/about/Biochar_dan_ Fungsionalisasi_Biochar.html?id=snLcDwAAQB AJ&redir_esc=y

[28] Setianingsih, T., Purwonugroho, D., Prananto, Y.P., Influence of Pyrolysis Parameters Using Microwave toward Structural Properties of ZnO/CNS Intermediate and Application of ZnCr$_2$O$_4$/CNS Final Product for Dark Degradation of Pesticide in Wet Paddy Soil, *ChemEngineering, 5*(58), 1 - 21 (2021).

https://doi.org/10.3390/chemengineering5030058

[29] Marsh, H. and Reinoso, R., Activated Carbon, Elsevier Sci., USA (2006).

https://www.google.co.id/books/edition/Activated_C arbon/UaOXSk2vFVQC?hl=id&gbpv=1&dq=Ma rsh,+H.+and+Reinoso,+R.,+Activated+Carbon&p g=PA86&printsec=frontcover

[30] Huang, Y., Hu, S., Zuo, S., Xu, Z., Han, C., Shen, J., Mesoporous Carbon Materials Prepared from Carbohydrates With A Metal Chloride Template, *J.Mater.Chem., 19*, 7759-7764 (2009).

https://doi.org/10.1039/B911011A

[31] Almawgooda, O.M.A., Tohamya, S.A.E., Ismail, E.H., Samhan, F.A., Sugarcane Bagasse Biochar with Nanomagnetite: A novel Composite Heavy Metals Pollutants Removal, *Egypt. J. Chem., 64*(3), 1293-1313 (2021).

doi: 10.21608/EJCHEM.2020.43158.2870

[32] Tsaneva, V.N., Kwapinski, W., Teng, X. Glowack, B.A., Assessment of The Structural Evolution of Carbons from Microwave Plasma Natural Gas Reforming and Biomass Pyrolysis Using Raman Spectroscopy, *Carbon, 80,* 617– 628 (2014).

https://doi.org/10.1016/j.carbon.2014.09.005

[33] Dhand, V., Hong, S.K., Li, L., Kim, J.M., Kim, S.H., Rhee, K.Y., Lee, H.W., Fabrication of Robust, Ultrathin and Light Weight, Hydrophilic, PVDF-CNT Membrane Composite for Salt Rejection, *Composites Part B, 160*, 632–643 (2019).

https://doi.org/10.1016/j.compositesb.2018.12.106

[34] Shriver, D.F., Atkins, P.W., Langford, C.H., Inorganic Chemistry, Oxford University Press, New York, 342 (1990).

[35]Young, R.O., (2016), Colloids and Colloidal Systems in Human Health and Nutrition, *International Journal of Complementary & Alternative Medicine, 3*(6), 1-8, DOI: 10.15406/ijcam 2016.03.00095

[36] Sinko, P.J., Singh. Y., Health, W.K., Martin's Physical Pharmacy and Pharmaceutical Sciences: physical, chemical and biopharmaceutical principles in the pharmaceutical sciences. 6th edition, Lippincott Williams & Wilkins, Philadelphia, 1-3 (2006).

https://innocentbalti.files.wordpress.com/2015/01/ma rtins-physical-pharmacy-6th-ed-2011-dr-murtadha-alshareifi.pdf

[37] Danby, J.M.A., Mashhoon, B., Safko, J.L., Gravitation, AccessScience from McGraw-Hill Education, 1-16 (2017).

https://www.accessscience.com/media/EST/media/29 8900PV0002.pdf

_____